

Spatial Pattern Assessment of Dengue Fever Risk in Subtropical Urban Environments: The Case of Hong Kong

1. Shi YIN ^{a,b}, aryinshi@hku.hk
2. Junyi HUA ^{c, *} huajunyi@ouc.edu.cn
3. Chao REN ^{a, *} renchao@hku.hk
4. Runxi Wang ^d runxiwg@connect.hku.hk
5. André Ibáñez Weemaels^d andribawe@gmail.com
6. Benoit Guénard ^d zeroben@gmail.com
7. Yuan SHI ^e, Yuan.Shi@liverpool.ac.uk
8. Tsz-Cheung LEE ^f tclee@hko.gov.hk
9. Hsiang-Yu YUAN ^g, sean.yuan@cityu.edu.hk
10. Marc Ka-chun CHONG ^h, marc@cuhk.edu.hk
11. Linwei TIAN ⁱ, linweit@hku.hk

^a Faculty of Architecture, The University of Hong Kong, Pokfulam, Hong Kong SAR, China

^b School of Architecture, South China University of Technology, Guangzhou, China

^c School of International Affairs and Public Administration, Ocean University of China, Qingdao, China;

^d School of Biological Sciences, The University of Hong Kong, Hong Kong SAR, China

^e Department of Geography and Planning, University of Liverpool, United Kingdom

^f Hong Kong Observatory, Hong Kong SAR, China

^g Department of Biomedical Sciences, City University of Hong Kong, Kowloon, Hong Kong SAR, China

^h JC School of Public Health and Primary Care, The Chinese University of Hong Kong, Hong Kong SAR, China

ⁱ School of Public Health, LKS Faculty of Medicine, The University of Hong Kong, Pokfulam, Hong Kong SAR, China

* Corresponding authors at:

Junyi HUA: School of International Affairs and Public Administration, Ocean University of China, Qingdao, Shandong Province, China, 266100

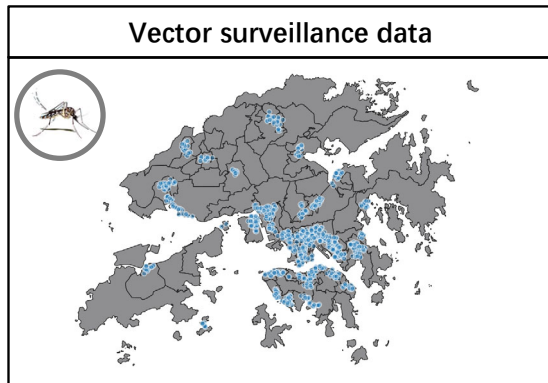
Chao REN: 6/F, Knowles Building, Faculty of Architecture, The University of Hong Kong, Pokfulam, Hong Kong SAR, China

Highlights

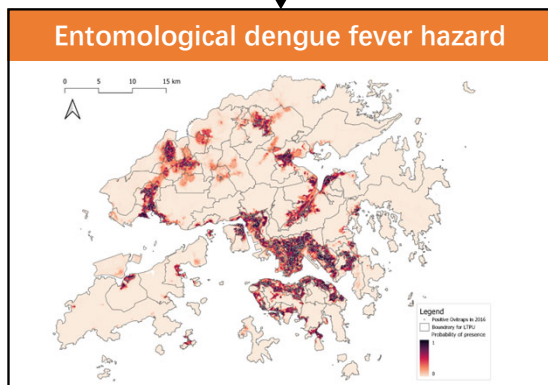
- Landscape metrics applied for assessing entomological dengue fever hazard
- Dengue fever risk is evaluated by adopting the IPCC's risk conceptual framework.
- Seventeen potential hotspots for dengue fever risk are identified in Hong Kong.
- The underlying factors responsible for hotspots are analyzed and discussed.
- Dengue fever risk maps are developed for local public health actions and planning.

Abstract

Dengue fever, a mosquito-borne fatal disease, brings a huge health burden in tropical regions. With global warming, rapid urbanization and the expansion of mosquitoes, dengue fever is expected to spread to many subtropical regions, leading to increased potential health risks on local populations. So far, limited studies assessed the dengue fever risk spatially for subtropical non-endemic regions hindering the development of related public health management. Therefore, we proposed a spatial hazard-exposure-vulnerability assessment framework for mapping the dengue fever risk in Hong Kong. Firstly, the spatial distribution of the habitat suitability for *Aedes albopictus*, the mosquito proxy for the dengue fever hazard, was predicted using a species distribution model (e.g., MaxEnt) relying on a list of variables related to local climate, urban morphology, and landscape metrics. Secondly, the spatial autocorrelation between high dengue hazard and high human population exposure in urban areas was measured. Finally, the dengue fever risk was assessed at community scale by integrating the results of vulnerability analysis basing on census data. This approach allowed the identification of 17 high-risk spots within Hong Kong. The landscape metrics about land utilities and vegetations, and urban morphological characteristics are the influential factors on the spatial distribution of dengue vector. In addition, the underlying factors behind each hot spot were investigated, and specific suggestions for dengue prevention were proposed accordingly. The findings provide a useful reference for developing local dengue fever risk prevention measures, with the proposed method easily exportable to other high-density cities within subtropical Asia and elsewhere.

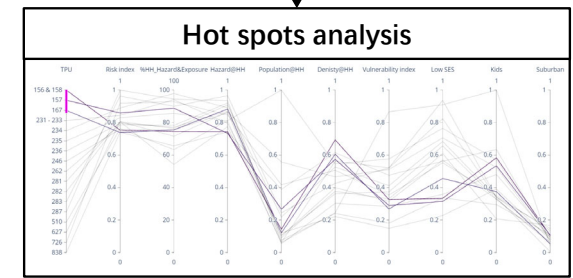
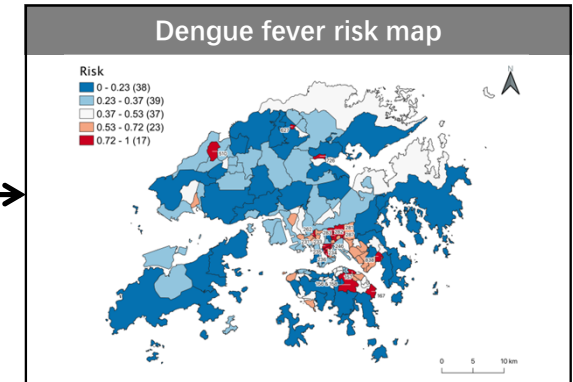
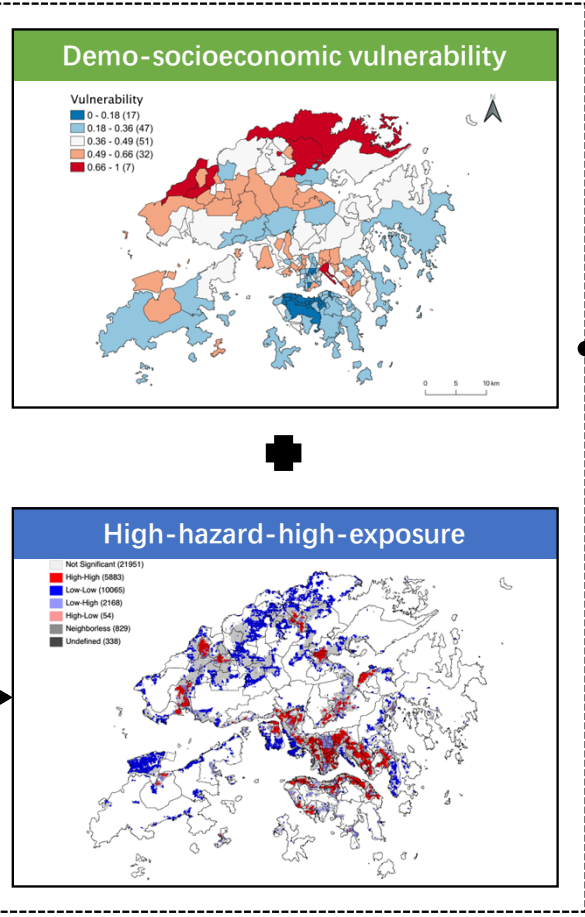


MaxEnt model



Population data from *WorldPop*

Local Moran's I



1 Introduction

2 Dengue fever (DF) is one of the most serious viral infectious diseases and is prevalent
3 across tropical and subtropical regions. The dengue virus (DENV) mainly spreads to
4 people through the bites of infected female mosquitoes of the genus *Aedes* with *Ae. aegypti*
5 and *Ae. albopictus* (Lambrechts et al., 2011). *Ae. aegypti* is featured as an endophilic species,
6 thus the highly urbanized area and indoor environment are favoured to them. Conversely, *Ae.*
7 *albopictus* is exophilic and prefers an outdoor environment with natural elements (Honório
8 et al., 2009). Globally, DF brings a vast health burden to human societies, with about half
9 of the world's population at risk and an estimated 100 to 400 million infections annually (Bhatt
10 et al., 2013). The DF risk is expected to rapidly grow globally relating to climate change, fast
11 urbanization, and international mobility (Romanello et al., 2021). Global warming and
12 increasing precipitation over land result in a significant sprawl of suitable regions for *Aedes*
13 mosquitoes (Kamal et al., 2018). In addition, fast urbanization might generate high
14 demographic regions with disproportionate infrastructure quality (Gubler, 2011). Both the
15 frequent human activities and the low-grade infrastructures might associate with
16 numerous unmanaged and semi-permanent garbage collections for holding water, which
17 facilitate mosquito breeding and production of biting adults resulting in increased risks of DF
18 transmission (LaDeau et al., 2013). Meanwhile, globalization facilitates international exchanges
19 and the spread of DENV into non-endemic regions. By 2080, the dengue burden could impact an
20 additional 2.25 billion people in the subtropical areas (Messina et al., 2019).

21 To comprehensively assess the risk of climate change impact, the Intergovernmental Panel
22 on Climate Change (IPCC) proposed a framework from three components, namely hazardous

23 events, exposure, and vulnerabilities (IPCC, 2014) to measure the potential for adverse
24 consequences. This framework is similar to the concept of Crichton's Risk Triangle (Crichton,
25 1999) and extendedly applied to assessing the risk from heat, flood, and so on (Hagenlocher et al.,
26 2019; Hua et al., 2021). As one of the climate-sensitive infectious diseases, limited studies have
27 assessed the DF risk following the risk triangle conceptual framework.

28 Though there is rich literature on assessing the DF risk spatially, most studies predicted the
29 likelihood of dengue transmission incidents in the endemic region (Yin et al., 2022). However,
30 understanding the spatial pattern of DF risk in *Aedes* mosquito domesticated but non-endemic
31 urban areas might be more valuable. On the one hand, the DENV transmission chain entirely
32 depends on the *Aedes* mosquitoes. Understanding the distribution of habitat suitability for *Aedes*
33 mosquitoes could inform the development of efficient strategies for the abundance of these
34 populations. Therefore, the abundance of these vectors is paramount in evaluating the DF risk
35 within non-endemic regions(Wiese et al., 2019). On the other hand, in the region where local
36 DENV transmissions are driven mainly by imported cases, like Hong Kong (Yuan et al., 2020),
37 there is no clear seasonality, and sufficient local infections can be observed for a prediction. Hence,
38 the outcome of DF risk assessment can support early plan control measures for preventing local
39 DF transmission.

40 Here, we propose a practical framework to assess the DF risk spatially in a subtropical
41 high-density city, with Hong Kong as a case study. The IPCC's risk concept is referred to and
42 applied in this study for assessing the DF risk from three perspectives, namely hazard, exposure,
43 and vulnerability. This study first develops a predictive spatial distribution model for the dengue
44 vectors based on surveillance data. After assessing the hazard, exposure, and vulnerability of DF
45 risk spatially, the DF risk in Hong Kong is mapped out. Finally, corresponding recommendations

46 and measures for controlling DF transmission are proposed according to the identified underlying
47 factors behind hot spots of DF risk. The findings of this study are expected not only to help relevant
48 stakeholders to identify areas presenting high DF risks and their associated factors but also to assist
49 DF control-related policymaking and action development.

50

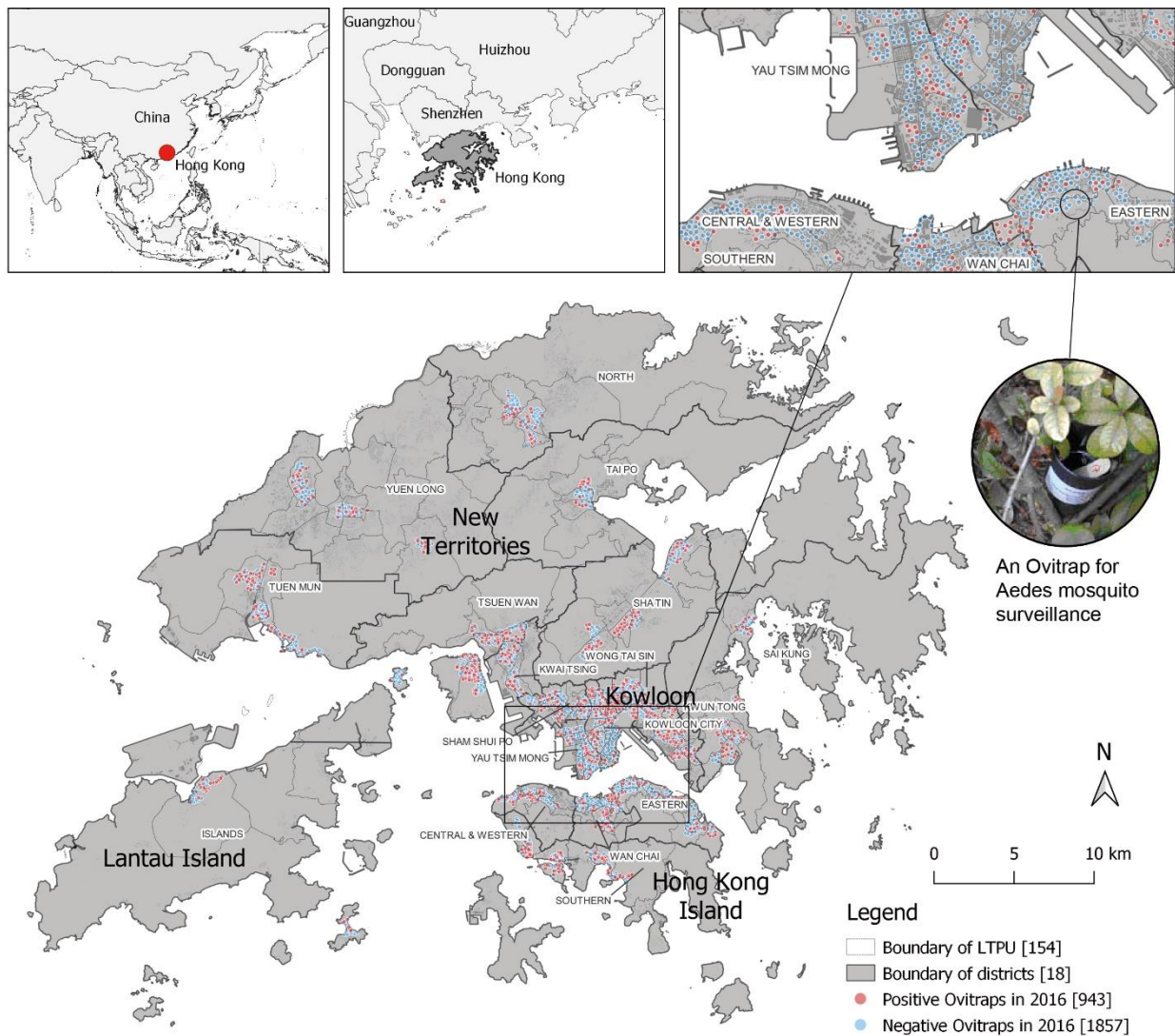
51 **2 Methodology**

52 *2.1 Study area and period*

53 The whole territory of the Hong Kong Special Administrative Region of the People's
54 Republic of China, located at the southern edge of the Sino-Japanese realm adjacent to the Oriental
55 realm, is selected as the case in our study (Figure 1). The city is famous for its high-density built
56 environment and population. Over seven million residents live in approximately 1113.76 km², of
57 which only 24 % is built-up land, and 7% is for residential purposes. On average, it causes a high
58 population density of about 26000 people/km² in built-up areas (CenStatD, 2022).

59 Despite being non-endemic for DF over the years, Hong Kong is under the constant threat
60 of a DF outbreak. At first, the climate of Hong Kong is characterized by hot and humid summers
61 and relatively milder winters, encouraging mosquito breeding. Against the background of climate
62 change and local urbanization, in the last century, Hong Kong has experienced a significant long-
63 term warming trend with more frequent and intense hot weather as well as prolonged summers
64 (Chan et al., 2012); Secondly, Hong Kong is facing the challenges of an ageing society and
65 expanding socioeconomic disparity (Wu, 2009). The city might become more vulnerable to DF in
66 the future as elderly people are deemed a high- risk group for developing severe dengue infection
67 (Xiao et al., 2016). In addition, the low socioeconomic level may be associated with unsanitary

68 and poor living conditions which can promote mosquito reproduction directly and increase the DF
 69 risk indirectly (Hagenlocher et al., 2013). Thirdly, Hong Kong is a global transit hub for
 70 international travellers and is geographically close to hyperendemic areas in Southeast Asia. An
 71 increasing trend in DF incidence has been found since the first local outbreak in 2002. From 2013
 72 to 2019, Hong Kong recorded DF cases annually over 100, and the majority of incidents were
 73 imported cases (Centre for Health Protection, 2019). However, the number of infected cases sunk
 74 significantly after 2020 due to the limitation of international traveling during the period of the
 75 COVID-19 pandemic.



77 *Figure 1. The study area and the locations of positive Ovitrap in the year 2016 in Hong Kong.*

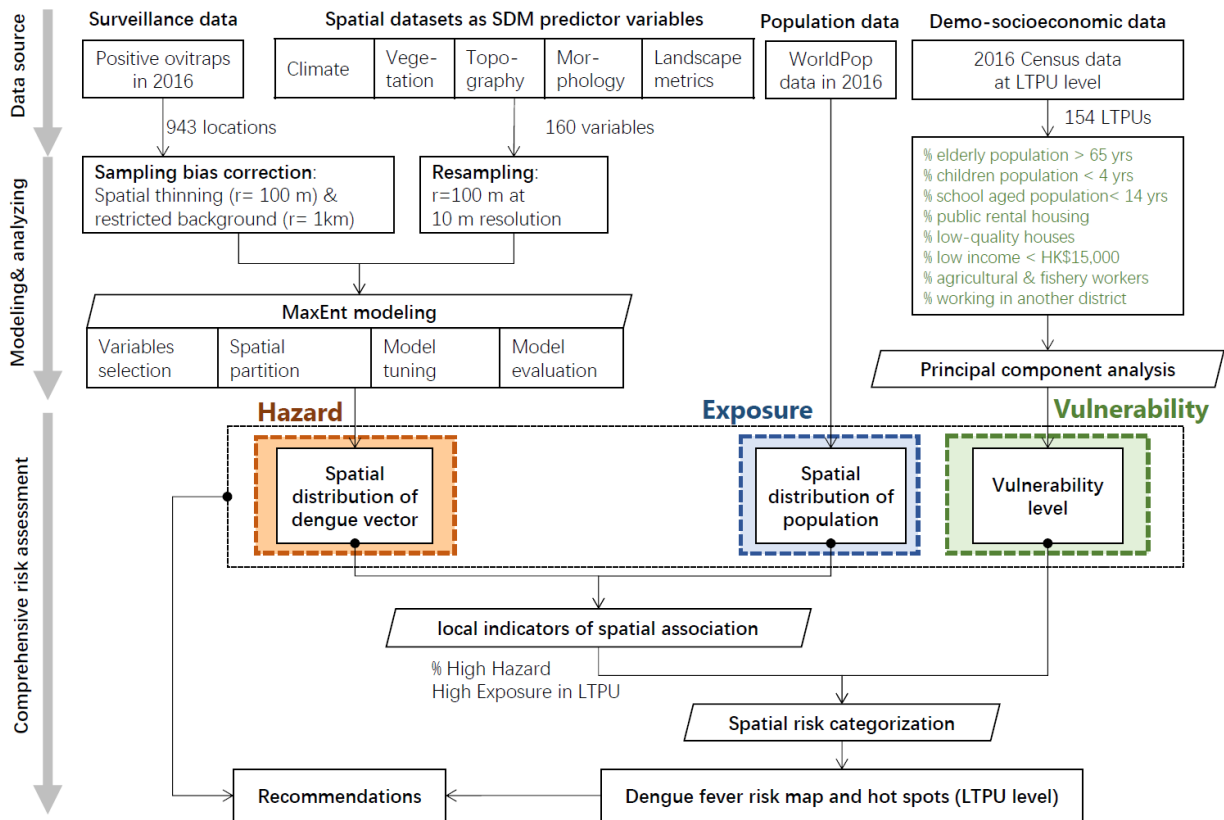
78 Since 2000, the Food and Environmental Hygiene Department of the Hong Kong
79 government has applied Oviposition Trap (Ovitrap) to detect the presence of adult *Aedes*
80 mosquitoes in urban areas (Wong et al., 2011). In Hong Kong, the *Ae. aegypti* is not found, but the
81 *Ae. albopictus* is abundant locally. An Ovitrap is a simple device made up of a black plastic
82 container of 200 ml capacity filled with water and a brownish oviposition paddle placed diagonally
83 inside. The Ovitrap were collected seven days after setting and then incubated for seven days
84 under controlled laboratory conditions. An Ovitrap is recorded as positive if any eggs or larvae of
85 *Ae. albopictus* is found after incubation. The surveillance data from Ovitrap supports the relevant
86 department in monitoring the abundance of DF vectors across Hong Kong and encourage public
87 participation in preventive measures.

88 The high urbanization ratio and relative feebly annual weather variability in Hong Kong
89 resulted in stable environmental suitability for dengue vectors. The official census data for 2016
90 are available. Therefore, we selected the year 2016 as the study period for assessing the DF risk
91 distribution across Hong Kong.

92 *2.2 Framework for risk assessment*

93 The conceptual framework of IPCC's risk assessment (IPCC, 2014) is adopted to develop
94 the DF risk maps in Hong Kong. The framework presents a concise structure of risk in three
95 separate dimensions, namely hazard, exposure, and vulnerability. Figure 2 presents the workflow
96 of this study: Firstly, various types of data are collected from multiple sources; secondly, the
97 distribution of the *Ae. albopictus* in Hong Kong is predicted by modelling based on surveillance
98 data cooperating with meteorological and environmental factors. The probability of vector
99 presence is a proxy of the entomological hazard of DENV transmission between residents. Then,

100 the local indicators of spatial association between hazard and exposure are calculated at
 101 Large Tertiary Planning Unit (LTPU) level. The vulnerability index for each LTPU comes
 102 from the principal component analysis (PCA) results on demo-socioeconomic characteristics.
 103 In the third step, the components of hazard, exposure, and vulnerability are integrated with equal
 104 weights for mapping the DF risk in Hong Kong, because there has been no agreement on the
 105 component weights in literature (Zhang et al., 2019). Finally, recommendations for the hot spots
 106 with DF risk in Hong Kong accordingly.



107
 108 *Figure 2. Workflow of the DF risk mapping*

109 **2.3 Data**

110 The study relies on four types of geo-coded data. The data availability and collection
 111 methods are shown below:

112 2.3.1 Ovitrap data

113 The dengue vector surveillance data in 2016 is offered by Food and Environmental
114 Hygiene Department (FEHD). FEHD selected 50-55 sites to set up ovitraps equidistantly (around
115 a hundred meters) at the height of closing to the ground surface within each of the 57 surveillance
116 areas. The selected surveillance areas are featured with higher human concentrations and potential
117 mosquito activities following the advice of the World Health Organization (WHO, 1995). In total,
118 2800 ovitraps were geocoded and collected monthly, and 943 sites were positive at least once in
119 2016.

120 2.3.2 meteorological and environmental data

121 In total, 160 meteorological and environmental variables of Hong Kong from three distinct
122 open data sources are employed in this study (Appendix A). The climate, vegetation, and
123 topography data are collected from a set of 30-m resolution rasters developed by Morgan and
124 Guénard (2019), including 27 climatic variables, Normalized Difference Vegetation Index (NDVI),
125 and 17 topographic variables.

126 Four class-level landscape metrics are selected to represent the spatial pattern of the 17
127 types of land use/landscape classes in Hong Kong (Appendix B). The class-level metrics are the
128 percentage of landscape types, largest patch index, aggregation index, and connectance index. 2
129 more widely used landscape-level metrics are included: One is the contagion index for
130 quantifying the degree of clumpiness of overall landscape patterns. Another one is the
131 Shannon's evenness index, for measuring the diversity of land use or landscape composition. In
132 total, 110 landscape metrics are retrieved from Shi et al. (2019) at a 10-m resolution. In
133 addition, six building morphological factors at a resolution of 10m are extracted from Shi et al.
(2018).

134 2.3.3 Gridded population data

135 For analyzing the spatial autocorrelation of hazard and exposure, the 100-m resolution
136 gridded estimates of the entire population in Hong Kong for the year 2016 are freely collected
137 from the WorldPop (www.worldpop.org) (Tatem, 2017).

138 2.3.4 Population census data

139 The demographic and socioeconomic data involving population segmentations by age,
140 education, income, occupation, housing status, etc., and population density at the Tertiary Planning
141 Unit (TPU) level based on the 2016 census – which are open access data on the websites
142 maintained by the Census and Statistics Department of the Hong Kong government (CenStatD,
143 2017).

144 2.4 Entomological DF hazard modelling

145 The maximum entropy (MaxEnt) algorithm is used for modeling the spatial distribution of
146 the dengue vector (Steven J. Phillips et al., 2017). MaxEnt, as the most widely used species
147 distribution model, has been described as especially efficient at handling complex interactions
148 between predicted species and predictors (Elith et al., 2011). The *ENMeval* package (Kass et al.,
149 2021) in *R* is applied for developing, evaluating, and tuning the MaxEnt models through the Java
150 software ‘maxent.jar’ (v 3.4.3). Optimization of the model is important for avoiding misleading
151 results and model overfitting (Merow et al., 2013). The MaxEnt model for the distribution of *Ae.*
152 *albopictus* in Hong Kong is developed following the process below:

153 2.4.1 Data preprocess

154 Considering that the *Aedes* mosquitoes will only fly within a few blocks in their whole
155 lifetime (Reiter et al., 1995), we set a buffer radius of 100 m for extracting urban environmental
156 data to explain the flight range of vectors. All predictor variables included are resampled at a 10-
157 m resolution by the moving window method, with the buffer using the *focalWeight* and *focal*
158 functions in the *raster* R package (Hijmans, 2019).

159 As a presence-only model, sampling bias significantly impacts models' performance (S. J.
160 Phillips et al., 2009). For correcting sampling bias, the *thin* function in the *Red* R package is applied
161 to limit the minimum distance between any occurrence at 100 m. Additionally, the selection of
162 background points may strongly affect the resulting model (Barve et al., 2011). As the ovitraps
163 were concentrated in the built area, but lacked surveillance data in the non-urbanized regions, we
164 extracted the pseudo-absences points within buffer areas with a 1 km radius around all occurrences
165 (see Appendix C).

166 2.4.2 Variables Selection

167 To avoid the model overfitting by the large number and collinearity of predictors, a full
168 MaxEnt model with all variables by default settings is first to run. The Spearman's correlation
169 coefficient between any predictors is calculated and a threshold value is set at 0.7. If any two
170 variables are found correlated above the threshold, the one having the least permutation importance
171 in the initial MaxEnt model is omitted. Then, only the predictor with a percentage contribution or
172 permutation importance of over 2% is remained for reducing the complexity of the final model.

173 2.4.3 Model tuning and evaluation

174 For averting spatial autocorrelation resulting from spatial clustering of large occurrence
175 points (Roberts et al., 2017), the 'Checkerboard2' spatial cross-validation method is employed for

176 generating 4 folds from the datasets. The regularization multiplier and feature classes are the two
 177 tuning parameters in optimizing the final MaxEnt model. The feature classes determine the
 178 potential shape of the marginal response curves, including Linear (L), Quadratic (Q), Hinge (H),
 179 Product (P), and Threshold (T). In our study, a total of 25 different models are evaluated by using
 180 multiple combinations of five feature classes (i.e., L, LQ, LQH, LQHP, and LQHPT) and five
 181 regularization multiplier values (i.e., 1 to 5).

182 For seeking the reliability of MaxEnt models, we use four metrics to evaluate the model
 183 performance, including the area under the curve (AUC) of the receiver operating characteristic
 184 curve for test localities (AUC_{TEST}), the difference between training and testing AUC (AUC_{DIFF}),
 185 and two different threshold-based omission rates for test localities, namely the omission rate of
 186 testing localities at the 10% training threshold (OR_{10P}) and the omission rate of training locality
 187 with the lowest value or the minimum training presence (OR_{MTP}) (Peterson et al., 2011). The Pareto
 188 frontiers between the averaged AUC_{TEST} and the other three evaluation metrics are computed by
 189 the *rprefR* package (Roocks, 2016) for selecting the optimal model following the criteria in Table
 190 1. Finally, the permutation importance of each variable in the optimal model and the response
 191 curves of the variables were further analyzed.

192 *Table 1. The evaluation metrics and criteria for selecting the optimal model*

Metrics	Evaluation Criteria	References
AUC_{TEST}	the output showing $0.5 < AUC \leq 0.7$ is considered failed or bad predictive power; $0.7 < AUC \leq 0.8$ is general; $0.8 < AUC \leq 0.9$ is good; $0.9 < AUC \leq 1.0$ is very good.	(Peterson et al., 2011)
AUC_{DIFF}	Value AUC_{DIFF} is expected to be positively associated with the degree of model overfitting	(Warren & Seifert, 2011)
OR_{10P}	Omission rates greater than the expectation of 10% typically indicate model overfitting	(Fielding & Bell, 1997;
OR_{MTP}	Omission rates greater than the expectation of zero typically indicate model overfitting	Peterson et al., 2011)

193 2.5 Statistical analysis for risk assessment

194 Unlike the entomological DF hazard and exposure that are evaluated at the grid level in a
195 fine resolution, the demo-socioeconomic data applied for assessing vulnerability are only collected
196 at the large Tertiary Planning Unit (TPU) level, according to the 2016 Census data. In total, 154
197 large TPUs (LTPUs) are defined within the whole territory of Hong Kong by the Planning
198 Department for urban planning and management purposes, delineating the nature of geographic
199 and zoning boundaries (Housing & Bureau, 2004).

200 However, the sizes of LTPUs are not equal and vary significantly. More importantly, the
201 radius of *Aedes* mosquitoes' foraging activities is around a few hundred meters (Sallam et al.,
202 2017). To assess the DF risk at the TPU level correctly, we focus on areas that simultaneously suit
203 *Aedes* mosquito breeding and contain dense populations in each LTPU instead of separately
204 considering the two aspects at the LTPU scale.

205 Therefore, the components of hazard and exposure are integrated by using local indicators
206 of spatial association (LISA) (Anselin, 1995) for identifying areas with a high level of hazard and
207 a high level of exposure (HH hazard-exposure). The proportion of HH hazard-exposure areas in
208 each TPU is calculated as a sub-index for assessing the composite DF risk.

209 2.5.1 High-hazard-high-exposure areas identification

210 The bivariate local Moran's I is utilized to identify clusters in terms of the spatial
211 autocorrelation between mosquito presence and population exposure (Anselin & Getis, 1992). The
212 technique has been utilized to study population exposure to natural hazards (Ge et al., 2021; Rinner
213 et al., 2010). The 10-m-resolution mosquito presence raster objects were resampled to the 100-m-
214 resolution population grids for the LISA. The high-high (HH) cluster of grids is detected as a high-

215 risk area. The proportion of the area of HH grids to the whole area is calculated for each LTPU as
216 a sub-index integrating hazard and exposure.

217 2.5.2 Principal component analysis of vulnerability-related information

218 We identified nine heat-vulnerability-related indicator variables based on the literature
219 review and the availability of Hong Kong census data. We extracted the data from the 2016 Census
220 at the TPU level for this study (Table 2). Then, the principal component analysis (PCA) is applied
221 for extracting the main components among the variables. Principal components with eigenvalues
222 above one are kept for a varimax rotation to derive orthogonal factors. A composite vulnerability
223 sub-index is calculated as the sum of the products of each factor score weighted by the
224 corresponding variance explained.

225 *Table 2. Vulnerable groups for dengue fever transmission in Hong Kong.*

No.	Vulnerable groups	Reasons	Abbr.	References
1	Population aged 65 and above	sensitive to co-morbidity	elderly_p	(de Mattos Almeida et al., 2007)
2	Population aged 4 and below	weaker immune systems	kid04_p	(Dickin et al., 2013)
3	Population aged 5-14	more likely to expose to mosquitoes	kid514_p	(Dickin et al., 2013)
4	Domestic households living in public rental housing units	low socioeconomic status with low living conditions	prh_p	(Akter et al., 2017)
5	Domestic households living in low-quality houses	less protective from mosquitoes	lowhou_p	(Dickin et al., 2013)
6	Population aged 15 and above with no schooling, pre-primary or primary education attainment	less knowledge and weaker awareness of self-protection	lowedu_p	(Dickin et al., 2013)
7	Domestic households with monthly income lower than HK\$15,000	less economically capable of protecting themselves and seeking medical help	lowinc_p	(Akter et al., 2017)
8	Working population as agricultural and fishery workers	probably working in high-hazard areas	agri_fish_p	(Akter et al., 2017)
9	Working population working in another district	higher exposure possibilities during commute	cross_dis_p	(Wijayanti et al., 2016)

226

227 **2.5.3 Risk assessment map and hot spots**

228 The DF risk assessment map is developed by overlapping the layer of hazard-exposure and
 229 vulnerability for calculating the risk index and map at the LTPU level. The weights of the three
 230 components are equal in the comprehensive risk assessment process. Considering the hazard and
 231 exposure are being integrated into a component rather than separated, the weights for the level of
 232 HH hazard and exposure account for 2/3, and 1/3 for vulnerability. After categorizing the risk
 233 levels into five by natural breaks, the LTPUs in the highest risk level is considered as hot spots.
 234 Finally, the underlying factors responsible for each hot spot are identified by analyzing the results
 235 of hazard, exposure, and vulnerability.

236 **3 Results**

237 *3.1 Spatial distribution of entomological DF hazard*

238 3.1.1 Variable selections

239 In the first round of variable selection, a total of 122 variables were excluded. In the second
240 step, there are 9 predictor variables with permutation importance of over 2%. The spearman's
241 correlation coefficient between any pair of predictor variables for modelling after this selection
242 process is shown in Appendix D. Six landscape metrics are detected as the important predictor for
243 mapping the spatial distribution of *Ae. Albopictus*.

244 3.1.2 Optimal model

245 Table 3 demonstrates the five models which are presented in the 3 Pareto frontiers
246 (Appendix E). The models are labeled and named according to the feature classes(fc) and
247 regularization multiplier(rm). For instance, the model built in fc of LQH and rm in 2 is named as
248 fc.LQH_rm.2. The AUC_{TRAIN} of all trained models ranges from 0.847 to 0.864, the differences of
249 AUC_{TEST} are relatively small. Though the fc.LQHPT_rm.1 model has both the highest AUC_{TRAIN}
250 and AUC_{TEST}, its AUC_{DIFF} and OR_{10P} are also higher than the others, which implies the model
251 might be overfitted. Therefore, fc.LQH_rm.2 is selected as the optimal model due to its low
252 AUC_{DIFF} and omission rates.

253 *Table 3. The selected models with evaluation metrics.*

Models	fc	rm	AUC_{TRAIN}	AUC_{TEST}	AUC_{DIFF}	OR_{10P}	OR_{MTP}
fc.LQHP_rm.1	LQHP	1	0.857	0.844	0.014	0.127	0.001
fc.LQHPT_rm.1	LQHPT	1	0.864	0.845	0.022	0.145	0.004
fc.LQH_rm.2	LQH	2	0.847	0.841	0.009	0.110	0.001
fc.LQHP_rm.2	LQHP	2	0.852	0.843	0.012	0.113	0.002
fc.LQHP_rm.3	LQHP	3	0.849	0.842	0.011	0.109	0.001

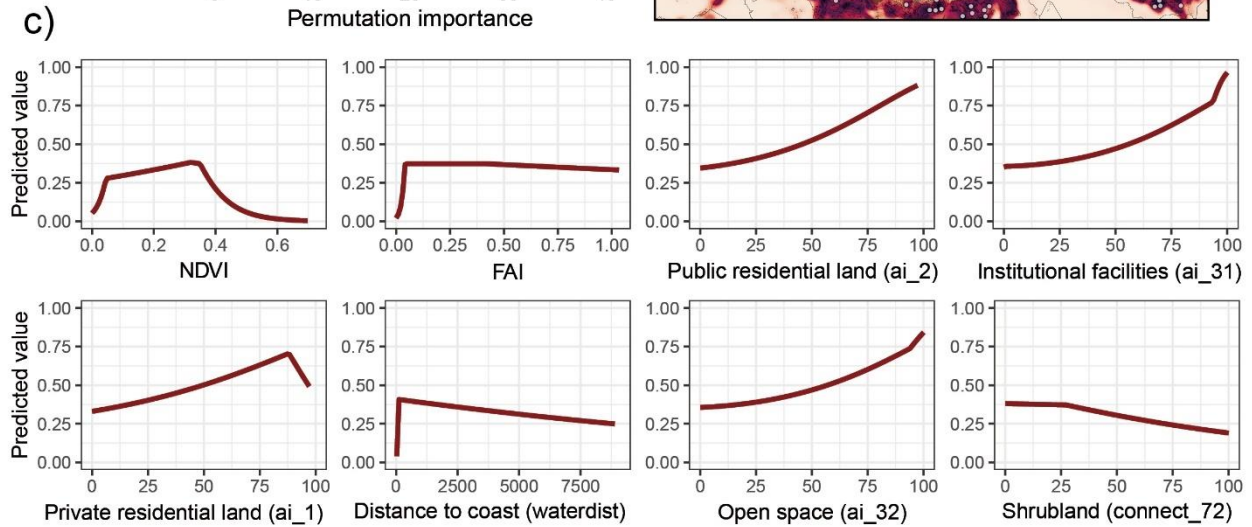
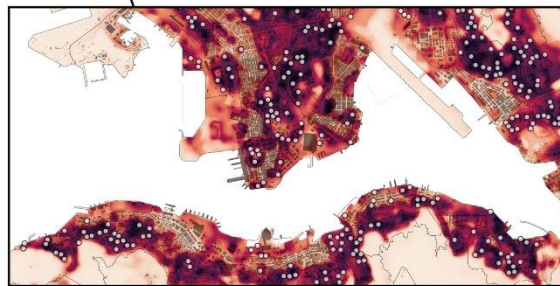
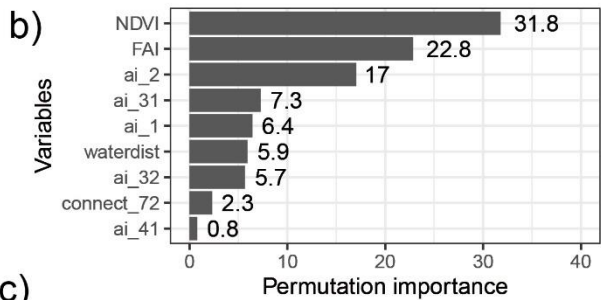
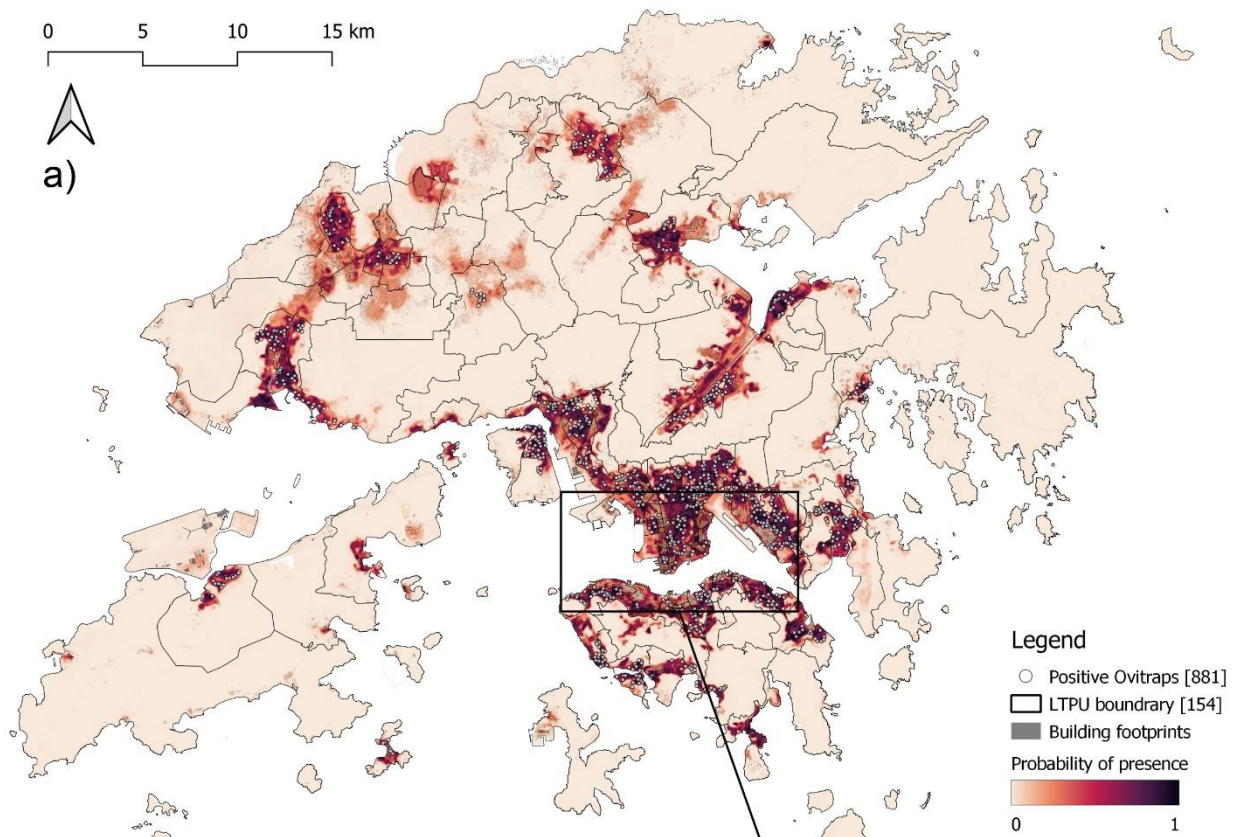
fc: Feature classes; rm: regularization multiplier

254 3.1.3 Spatial distribution and influential factors

255 In total, 843 positive Ovitrap traps remained after spatial thinning. Figure 3 demonstrates the
256 spatial distribution of the probability of *Ae. albopictus* presence in Hong Kong. High probabilities
257 are concentrated in built-up areas. Several areas with high levels of hazards were not included as
258 surveillance regions.

259 According to the permutation importance of all selected variables, the NDVI, FAI (total
260 frontal area of all buildings in the urban lot along with the wind direction), and the aggregation
261 index of public residential land (ai_2) rank the top three among all predictors, with permutation
262 importance of 31.8%, 22.8%, and 17% respectively. The aggregation index of roads (ai_41)
263 demonstrates hardly any influence on the suitability of the habitat of *Aedes* mosquito, only 0.8%.

264 In terms of the response curve, the NDVI, FAI, aggregation index of private residential
265 land (ai_1) and distance to coast (waterdist) demonstrate nonlinear relationships with the predicted
266 value. The predicted value peaks at 0.35 for NDVI, and 87.5 for the aggregation index of private
267 residential land (ai_1). Conversely, the aggregation index of public housing (ai_2), institutional
268 facilities (ai_31), and open space (ai_32) is associated with the probability of *Aedes* mosquito
269 presence positively in the shape of an exponent. In general, the suitable habitats for *Ae. albopictus*
270 in Hong Kong are close to water or shrublands, located in highly aggregated residential or public
271 facility lands, and covered by vegetation at medium level.



273 *Figure 3. Results of modeling on the spatial distribution of dengue vector. a) The map for the probability of Ae.*
274 *albopictus presence in Hong Kong; b) Permutation importance of predictor variables; c) Model response curves*
275 *of 8 environmental factors with permutation importance of over 2%. Red lines show averages after four*
276 *iterations of the model.*

277

278 3.2 Spatial pattern of DF risk

279 3.2.1 High hazard and high exposure areas

280 The distribution of the exposure-hazard level of LTPUs is displayed in Figure 4a. LTPUs
281 with at least two-thirds of their area in the HH class are mainly in the east of Hong Kong Island
282 and Kowloon. The global Moran's I is 0.563 with a z-value of 162.6. According to the LISA cluster
283 map, 14.2% of the total grids fall into the HH class. Among the 154 LTPUs, the HH class accounts
284 for 29.8% ($\pm 26.6\%$) of the area on average, with 21 LTPUs having no HH grids (Appendix F).

285 3.2.2 PCA analysis and vulnerability distribution

286 The principal component analysis generates three components with eigenvalues over one.
287 The three components explain 75% of the total variance. Factor loadings are presented in Table 4.
288 The first factor mainly accounts for areas with people having low socioeconomic status (LowSES),
289 living in public rental housing, working in another district, and slightly covering more elderly
290 people. The second factor (Kids) represents areas with higher proportions of children under 14 and
291 fewer elderly people and people of low socioeconomic status. The third factor explains suburban
292 areas featured temporary quarters and agricultural and fishery workers (Suburban). Figure 4b
293 shows the distribution of integrated vulnerability. High-vulnerability LTPUs are mainly in the
294 north of the city, with one exception in Kowloon (Appendix G).

295

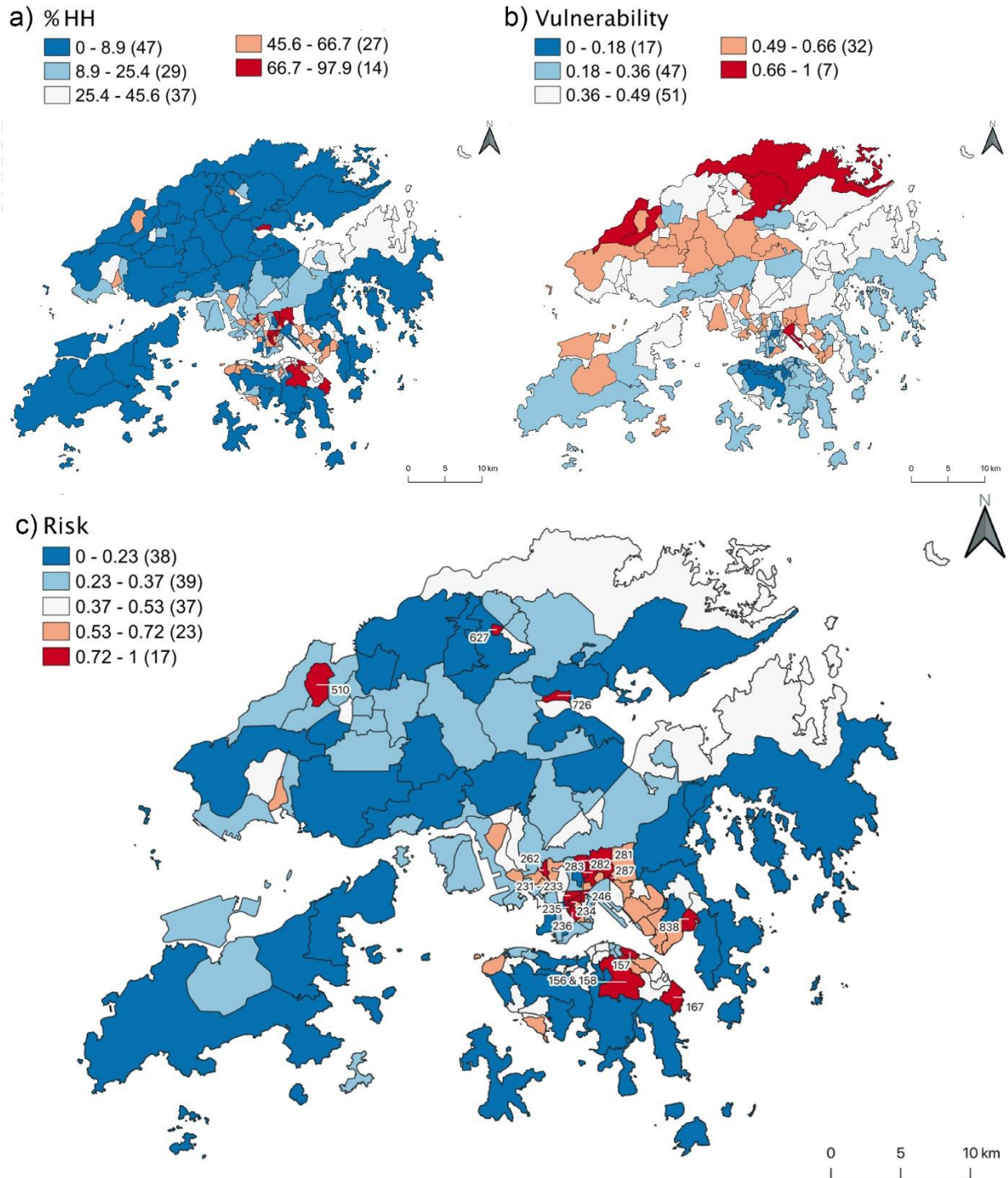
Table 4. PCA analysis on vulnerable groups

Variable	Factor1	Factor2	Factor3	Uniqueness
	LowSES	Kids	Suburban	
elderly_p	0.361	-0.796		0.193
kid04_p		0.771	0.360	0.247
kid514_p		0.807		0.332
prh_p	0.814		-0.339	0.197
lowhou_p			0.792	0.326
lowedu_p	0.794	-0.463		0.080
lowinc_p	0.722	-0.408		0.264
agri_fish_p			0.771	0.345
work_in_an~p	0.821			0.266
Eigenvalue	3.551	1.845	1.355	
% Variance explained	0.304	0.264	0.182	
Cumulative variance explained= 0.75				
Kaiser-Meyer-Olkin Measure of Sampling Adequacy= 0.702				
Chi-square= 700.032				
p-value= 0				

296

297 3.2.3 DF risk assessment map

298 Figure 4c illustrates the spatial distribution of DF risk in Hong Kong. In total, 17 LTPUs
 299 are categorized into the highest risk class with a risk index of over 0.72, and 23 LTPUs are
 300 considered to have moderate-high risk (0.53 - 0.72). LTPUs of relatively higher risks are mainly
 301 concentrated in the eastern parts of Hong Kong Island and Kowloon. There are three isolated spots
 302 in the northern territories of Hong Kong. The underlying factors behind the hot spots are analyzed
 303 according to the detailed results from the hazard, exposure, and vulnerability (See details in
 304 Appendix H). The



305

306 *Figure 4. Maps for dengue fever risk assessment in Hong Kong. a) Local indicators of spatial association of*
 307 *high hazard and high exposure; b) Spatial pattern of vulnerability; c) DF risk assessment map (the areas with*
 308 *the high DF risk level are labeled according to their codes of LTPU).*

309

310 **4 Discussion**

311 The hot spots identified in this study are consistent with the situation in 2018. In August
312 of that year, Hong Kong experienced its largest dengue outbreak so far. According to the
313 geolocation records, the biggest cluster of local dengue cases in 2018 was found in LTPU 282
314 and 283, namely the areas of Lion Rock Park and Wong Tai Sin. Additionally, the influential
315 factors on the spatial distribution of the dengue vector and the underlying drivers for hot spots
316 evaluated in the results support the recommendations regarding dengue fever prevention.

317 *4.1 Influential factors on the spatial distribution of dengue vector*

318 Though the climatic aspect is widely considered the primary inducement for mosquito
319 breeding, there are no climatic predictors are included in the optimal MaxEnt model. One potential
320 reason is that Hong Kong's climate suits mosquito breeding perfectly most of the time in a year,
321 where *Aedes* mosquito is present in the winter season with much lower abundance (Wong et al.,
322 2011). In addition, the spatial variability of climatic factors might be limited between urban regions
323 at a small scale, and climatic variables present significant multi-collinearity with topographic
324 features. For instance, the coefficient value between the annual average minimum air temperature
325 and distance to the coast (waterdist) is -0.75. Therefore, the information about topography might
326 be more critical than climatic factors for assessing mosquito presence within the urban
327 environment.

328 The nonlinear impact of NDVI and FAI on the *Aedes* mosquito abundance has been
329 extensively investigated(Kala et al., 2020). The life histories of *Ae. Albopictus* rely on both
330 vegetal food resources and human activities simultaneously. The areas without tall
331 vegetations or settlements seems to exclude *Ae. Albopictus* (Cox et al., 2007). Given that the
area with more

332 greenery usually implies less urbanized land, and vice versa, the high density of vegetation
333 coverage or urban areas illustrate negative impacts on the reproduction rates of dengue
334 vectors. Similar findings were reported by other studies in adjacent cities to Hong Kong, like
335 Guangzhou and Kaohsiung, where the risk of DF caused by *Ae. albopictus* increased in city
336 boundary and urban fringe areas, rather than the city center (Ren et al., 2017; Wen et al., 2015).

337 The landscape metrics play an important role in detecting the presence possibility of
338 dengue vector. The aggregation index of four types of land use and landscapes is positively related
339 to the suitability of habitat for *Aedes* mosquitoes. Residential land use is widely regarded as the
340 area preferred by *Aedes*, since there are adequate conditions for mosquito egg laying and larval
341 development, including artificial containers and vegetation (Little et al., 2017). The institutional
342 facilities (ai_31) and open space (ai_32) often refer to the crowd-gathering places, which are
343 adjacent to open space and landscape for assembling purposes, which suits well *Ae. albopictus*
344 breeding and foraging activities (Wen et al., 2015). Surprisingly, we found that the increase of
345 private housing aggregation (ai_1) reduces significantly the probability of *Ae. albopictus* presence.
346 A potential explanation may lie in the strong reduction or lack of vegetation in areas with an
347 extremely high proportion of private residential land. Conversely, the regulations on greening plot
348 areas in public housing land are restricted (Lee et al., 2019). Another potential reason is that the
349 measures taken in private housing estates to prevent mosquito breeding might be more frequent or
350 efficient, relating to better income levels and estate management (Gou et al., 2018).

351 *4.2 Underlying factors for hot spots and recommendations*

352 In the area featured with high population density and percentages of HH hazard-exposure area,
353 the probability of human-mosquito contact is significant and increases the potential for disease
354 transmission (Li et al., 2018). Therefore, the intensity of vector surveillance and mosquito control

355 management could be improved in these regions to avoid DENV transmission rapidly; In the area
356 with high LowSES, more efforts should be put into the general education of DF prevention for the
357 residents, so they can take corresponding actions at the individual level, such as adding window
358 screens, emptying and scrubbing containers, etc. For the LTPU with a high proportion of Kids,
359 more attention should be paid to the school environments during the period of the local DF
360 outbreak. Younger children have shown higher sensitivity to dengue transmission (Jain &
361 Chaturvedi, 2010). They are vulnerable to dengue transmission in school buses or yards during
362 early morning biting hours (Ooi et al., 2001).

363 *4.3 Implementations*

364 The findings of this study not only provide useful reference information for local government
365 bureaus to develop location-specific and cost-effective DF prevention measures but also serve as
366 an exemplary case for other subtropical high-density cities in DF preparedness. First, The fine-
367 resolution map of the suitable habitats of *Ae. albopictus* (Figure 3) might represent a valuable tool
368 for stakeholders at local level to find appropriate locations for setting mosquito traps, especially in
369 areas with low population density but high percentages of HH hazard-exposure area. Additionally,
370 the spatial pattern of DF risk in Hong Kong shows hot spots (Figure 4) and reasons behind each
371 high-level DF risk area (Appendix H), which are valuable knowledges and references for local
372 government and relevant departments to understand the composition of the risk and take action
373 accordingly.

374 Last but not least, the developed methodology and practical implications from this study could
375 be referred to by other municipal governments of subtropical high-density cities. Due to climate
376 change and urbanization, suitable habitats for dengue vectors will likely be enlarged globally,
377 potentially exposing more people to the risk of DF (Kamal et al., 2018). There is an urgent need

378 for these sub-tropical cities and regions to detect hot spots of DF risk and the underlying
379 determinants for better DF risk control towards healthy city development.

380 *4.4 Limitations and future works*

381 In this study, the hazard of DF risk is represented by the possibility of *Ae. albopictus*
382 presence rather than the abundance of adult *Aedes* mosquitoes. This limitation mainly relates to
383 that Ovitrap can only capture the egg and larvae from *Aedes* mosquitoes, instead of their adults. In
384 addition, the demographic and socioeconomic data are limited in LTPU scale. As the base unit for
385 assessing DF risk, the size of LTPU varies significantly between the core urban and suburban areas.
386 In the New Territories, some LTPUs are quite large but with fewer populations due to the presence
387 of country parks. Therefore, the precision of spatial assessment on vulnerability might be
388 restrained.

389 Future studies can apply new tools, like Gravidtrap, to replace the Ovitrap for monitoring
390 the population of adult dengue vectors and predicting the spatial pattern of entomological DF risk
391 more precisely. In addition, the spatial patterns of hazard, exposure, and vulnerability for DF risk
392 in Hong Kong might vary with time greatly due to climate change, aging society, and
393 socioeconomic disparity. Therefore, future works will also focus on both spatial and temporal
394 changes in DF risk under different scenarios. Through risk mapping and comprehensive
395 assessment, the findings can support public health management to prepare in advance for future
396 challenges.

397

398 **5 Conclusions**

399 This study developed a spatial assessment of DF risk by spatially integrating the DF-related
400 hazard, exposure, and vulnerability in the context of a high-density city in the sub-tropics, Hong
401 Kong. As Hong Kong is a non-endemic region for DF yet, the possibility of *Aedes* mosquito
402 presence is used as a proxy for the entomological DF hazard. The results of species distribution
403 model illustrate that the NDVI, FAI, and landscape metrics about residential, institutional facilities,
404 and open space land are the most significant influential factors on the spatial distribution of *Ae.*
405 *albopictus* in Hong Kong. The DF risk index is assessed at the LTPU level and 17 hot spots are
406 identified among about 150 census patches. Based on the underlying factors behind hot spots from
407 the aspects of hazard, exposure, and vulnerability, specific measures are proposed for preventing
408 DF transmission in corresponding LTPUs.

409 The information from the resultant models and maps benefits targeting neighbourhoods of
410 high risk and understanding the drivers behind the risk. The stakeholders and urban planners can
411 take action on precisely dealing with specific locations or residential areas to improve public health.
412 Additionally, the assessment framework developed in this study could also be referred to by other
413 municipality governments to analyze the risk of other vector-borne diseases, such as chikungunya,
414 yellow fever, and Zika, under the complex context of the metropolis spatially, to prepare for the
415 future challenges and to reduce potential negative impacts on public health.

Reference

- Akter, R., Naish, S., Hu, W., et al. (2017). Socio-demographic, ecological factors and dengue infection trends in Australia. *PLoS ONE*, 12(10), e0185551. <https://doi.org/10.1371/journal.pone.0185551>.
- Anselin, L. (1995). Local Indicators of Spatial Association-LISA. *Geographical Analysis*, 27(2), 93-115. <https://doi.org/10.1111/j.1538-4632.1995.tb00338.x>.
- Anselin, L., & Getis, A. (1992). Spatial statistical analysis and geographic information systems. *The Annals of Regional Science*, 26(1), 19-33. <https://doi.org/10.1007/BF01581478>.
- Barve, N., Barve, V., Jiménez-Valverde, A., et al. (2011). The crucial role of the accessible area in ecological niche modeling and species distribution modeling. *Ecological Modelling*, 222(11), 1810-1819. <https://doi.org/10.1016/j.ecolmodel.2011.02.011>.
- Bhatt, S., Gething, P. W., Brady, O. J., et al. (2013). The global distribution and burden of dengue. *Nature*, 496(7446), 504-507. <https://doi.org/10.1038/nature12060>.
- CenStatD. (2017). *Hong Kong 2016 population by-census main results*. Retrieved from: <https://www.byensus2016.gov.hk>. Accessed 2022-10-01
- CenStatD. (2022). *Hong Kong in Figures*. Retrieved from: <http://www.censtatd.gov.hk>. Accessed 2022-10-01
- Centre for Health Protection. (2019). *Number of notifiable infectious diseases by month*. Retrieved from: <http://www.chp.gov.hk>. Accessed 2022-08-30
- Chan, H. S., Kok, M. H., & Lee, T. C. (2012). Temperature trends in Hong Kong from a seasonal perspective. *Climate Research*, 55(1), 53-63. <https://doi.org/10.3354/cr01133>.
- Cox, J., Grillet, M. E., Ramos, O. M., et al. (2007). Habitat Segregation of Dengue Vectors Along an Urban Environmental Gradient. *The American Journal of Tropical Medicine and Hygiene*, 76(5), 820-826. <https://doi.org/10.4269/ajtmh.2007.76.820>.
- Crichton, D. (1999). The Risk Triangle. In J. Ingleton (Ed.), *Natural disaster management*. Leicester, England: Tudor Rose.
- de Mattos Almeida, M. C., Caiaffa, W. T., Assuncao, R. M., et al. (2007). Spatial vulnerability to dengue in a Brazilian urban area during a 7-year surveillance. *J Urban Health*, 84(3), 334-345. <https://doi.org/10.1007/s11524-006-9154-2>.
- Dickin, S. K., Schuster-Wallace, C. J., & Elliott, S. J. (2013). Developing a vulnerability mapping methodology: applying the water-associated disease index to dengue in Malaysia. *PLoS One*, 8(5), e63584. <https://doi.org/10.1371/journal.pone.0063584>.
- Elith, J., Phillips, S. J., Hastie, T., et al. (2011). A statistical explanation of MaxEnt for ecologists. *Diversity and Distributions*, 17(1), 43-57. <https://doi.org/10.1111/j.1472-4642.2010.00725.x>.
- Fielding, A. H., & Bell, J. F. (1997). A review of methods for the assessment of prediction errors in conservation presence/absence models. *Environmental conservation*, 24(1), 38-49. <https://doi.org/10.1017/S0376892997000088>.
- Ge, Y., Dou, W., Wang, X., et al. (2021). Identifying urban–rural differences in social vulnerability to natural hazards: a case study of China. *Natural Hazards*, 108(3), 2629-2651. <https://doi.org/10.1007/s11069-021-04792-9>.

- Gou, Z., Xie, X., Lu, Y., et al. (2018). Quality of Life (QoL) Survey in Hong Kong: Understanding the Importance of Housing Environment and Needs of Residents from Different Housing Sectors. *International Journal of Environmental Research and Public Health*, 15(2), 219. Retrieved from <https://www.mdpi.com/1660-4601/15/2/219>.
- Gubler, D. J. (2011). Dengue, Urbanization and Globalization: The Unholy Trinity of the 21(st) Century. *Trop Med Health*, 39(4 Suppl), 3-11. <https://doi.org/10.2149/tmh.2011-S05>.
- Hagenlocher, M., Delmelle, E., Casas, I., et al. (2013). Assessing socioeconomic vulnerability to dengue fever in Cali, Colombia: statistical vs expert-based modeling. *International Journal of Health Geographics*, 12(1), 36. <https://doi.org/10.1186/1476-072X-12-36>.
- Hagenlocher, M., Meza, I., Anderson, C. C., et al. (2019). Drought vulnerability and risk assessments: state of the art, persistent gaps, and research agenda. *Environmental Research Letters*, 14(8). <https://doi.org/10.1088/1748-9326/ab225d>.
- Honório, N. A., Castro, M. G., Barros, F. S. M. d., et al. (2009). The spatial distribution of *Aedes aegypti* and *Aedes albopictus* in a transition zone, Rio de Janeiro, Brazil. *Cadernos de Saúde Pública*, 25, 1203-1214. <https://doi.org/10.1590/s0102-311x2009000600003>.
- Housing, P., & Bureau, L. (2004). *Implementation of Data Alignment Measures for the Alignment of Planning, Lands and Public Works Data*. Retrieved from Hong Kong SAR: <https://www.devb.gov.hk>
- Hua, J., Zhang, X., Ren, C., et al. (2021). Spatiotemporal assessment of extreme heat risk for high-density cities: A case study of Hong Kong from 2006 to 2016. *Sustainable Cities and Society*, 64. <https://doi.org/10.1016/j.scs.2020.102507>.
- IPCC. (2014). *Climate Change 2014: Impacts, Adaptation, and Vulnerability. Part A: Global and Sectoral Aspect*. (Vol. Summary for Policymakers). Cambridge, United Kingdom and New York, NY, USA: Cambridge University Press.
- Kala, A. K., Atkinson, S. F., & Tiwari, C. (2020). Exploring the socio-economic and environmental components of infectious diseases using multivariate geovisualization: West Nile Virus. *PeerJ*, 8, e9577. <https://doi.org/10.7717/peerj.9577>.
- Kamal, M., Kenawy, M. A., Rady, M. H., et al. (2018). Mapping the global potential distributions of two arboviral vectors *Aedes aegypti* and *Ae. albopictus* under changing climate. *PLoS ONE*, 13(12), 21. <https://doi.org/10.1371/journal.pone.0210122>.
- Kass, J. M., Muscarella, R., Galante, P. J., et al. (2021). ENMeval 2.0: Redesigned for customizable and reproducible modeling of species' niches and distributions. *Methods in Ecology and Evolution*, 12(9), 1602-1608. <https://doi.org/10.1111/2041-210x.13628>.
- LaDeau, S. L., Leisnham, P. T., Biehler, D., et al. (2013). Higher mosquito production in low-income neighborhoods of Baltimore and Washington, DC: understanding ecological drivers and mosquito-borne disease risk in temperate cities. *Int J Environ Res Public Health*, 10(4), 1505-1526. <https://doi.org/10.3390/ijerph10041505>.
- Lambrechts, L., Paaijmans, K. P., Fansiri, T., et al. (2011). Impact of daily temperature fluctuations on dengue virus transmission by *Aedes aegypti*. *Proc Natl Acad Sci U S A*, 108(18), 7460-7465. <https://doi.org/10.1073/pnas.1101377108>.
- Lee, L. S. H., Jim, C. Y., & Zhang, H. (2019). Tree density and diversity in Hong Kong's public housing estates: From provision injustice to socio-ecological inclusiveness. *Urban Forestry & Urban Greening*, 46, 126468. <https://doi.org/10.1016/j.ufug.2019.126468>.

- Li, Q., Cao, W., Ren, H., et al. (2018). Spatiotemporal responses of dengue fever transmission to the road network in an urban area. *Acta Trop*, 183, 8-13. <https://doi.org/10.1016/j.actatropica.2018.03.026>.
- Little, E., Bajwa, W., & Shaman, J. (2017). Local environmental and meteorological conditions influencing the invasive mosquito *Ae. albopictus* and arbovirus transmission risk in New York City. *PLoS Negl Trop Dis*, 11(8), e0005828. <https://doi.org/10.1371/journal.pntd.0005828>.
- Merow, C., Smith, M. J., & Silander, J. A. (2013). A practical guide to MaxEnt for modeling species' distributions: what it does, and why inputs and settings matter. *Ecography*, 36(10), 1058-1069. <https://doi.org/10.1111/j.1600-0587.2013.07872.x>.
- Messina, J. P., Brady, O. J., Golding, N., et al. (2019). The current and future global distribution and population at risk of dengue. *Nat Microbiol*, 4(9), 1508-1515. <https://doi.org/10.1038/s41564-019-0476-8>.
- Morgan, B., & Guénard, B. (2019). New 30 m resolution Hong Kong climate, vegetation, and topography rasters indicate greater spatial variation than global grids within an urban mosaic. *Earth System Science Data*, 11(3), 1083-1098. <https://doi.org/10.5194/essd-11-1083-2019>.
- Ooi, E. E., Hart, T. J., Tan, H. C., et al. (2001). Dengue seroepidemiology in Singapore. *The Lancet*, 357(9257), 685-686. [https://doi.org/10.1016/s0140-6736\(00\)04137-4](https://doi.org/10.1016/s0140-6736(00)04137-4).
- Peterson, A. T., Soberón, J., Pearson, R. G., et al. (2011). Princeton: Princeton University Press.
- Phillips, S. J., Anderson, R. P., Dudík, M., et al. (2017). Opening the black box: an open-source release of Maxent. *Ecography*, 40(7), 887-893. <https://doi.org/10.1111/ecog.03049>.
- Phillips, S. J., Dudík, M., Elith, J., et al. (2009). Sample selection bias and presence-only distribution models: implications for background and pseudo-absence data. *Ecol Appl*, 19(1), 181-197. <https://doi.org/10.1890/07-2153.1>.
- Reiter, P., Amador, M. A., Anderson, R. A., et al. (1995). dispersal of *Aedes aegypti* in an urban area after blood feeding as demonstrated by rubidium-marked eggs. *The American journal of tropical medicine and hygiene*, 52(2), 177-179. <https://doi.org/10.4269/ajtmh.1995.52.177>.
- Ren, H., Zheng, L., Li, Q., et al. (2017). Exploring Determinants of Spatial Variations in the Dengue Fever Epidemic Using Geographically Weighted Regression Model: A Case Study in the Joint Guangzhou-Foshan Area, China, 2014. *Int J Environ Res Public Health*, 14(12). <https://doi.org/10.3390/ijerph14121518>.
- Rinner, C., Patychuk, D., Bassil, K., et al. (2010). The Role of Maps in Neighborhood-level Heat Vulnerability Assessment for the City of Toronto. *Cartography and Geographic Information Science*, 37(1), 31-44. <https://doi.org/10.1559/152304010790588089>.
- Roberts, D. R., Bahn, V., Ciuti, S., et al. (2017). Cross-validation strategies for data with temporal, spatial, hierarchical, or phylogenetic structure. *Ecography*, 40(8), 913-929. <https://doi.org/10.1111/ecog.02881>.
- Romanello, M., McGushin, A., Di Napoli, C., et al. (2021). The 2021 report of the Lancet Countdown on health and climate change: code red for a healthy future. *The Lancet*, 398(10311), 1619-1662. [https://doi.org/10.1016/s0140-6736\(21\)01787-6](https://doi.org/10.1016/s0140-6736(21)01787-6).

- Sallam, M. F., Fizer, C., Pilant, A. N., et al. (2017). Systematic Review: Land Cover, Meteorological, and Socioeconomic Determinants of Aedes Mosquito Habitat for Risk Mapping. *Int J Environ Res Public Health*, 14(10). <https://doi.org/10.3390/ijerph14101230>.
- Shi, Y., Ren, C., Lau, K. K.-L., et al. (2019). Investigating the influence of urban land use and landscape pattern on PM2.5 spatial variation using mobile monitoring and WUDAPT. *Landscape and Urban Planning*, 189, 15-26. <https://doi.org/10.1016/j.landurbplan.2019.04.004>.
- Shi, Y., Xie, X., Fung, J. C.-H., et al. (2018). Identifying critical building morphological design factors of street-level air pollution dispersion in high-density built environment using mobile monitoring. *Building and Environment*, 128, 248-259. <https://doi.org/10.1016/j.buildenv.2017.11.043>.
- Tatem, A. J. (2017). WorldPop, open data for spatial demography. *Scientific data*, 4(1), 1-4.
- Warren, D. L., & Seifert, S. N. (2011). Ecological niche modeling in Maxent: the importance of model complexity and the performance of model selection criteria. *Ecol Appl*, 21(2), 335-342. <https://doi.org/10.1890/10-1171.1>.
- Wen, T.-H., Lin, M.-H., Teng, H.-J., et al. (2015). Incorporating the human-Aedes mosquito interactions into measuring the spatial risk of urban dengue fever. *Applied Geography*, 62, 256-266. <https://doi.org/10.1016/j.apgeog.2015.05.003>.
- WHO. (1995). *Guidelines for dengue surveillance and mosquito control* (9290610689). Retrieved from http://apps.who.int/iris/bitstream/10665/207027/1/9290611383_eng.pdf
- Wiese, D., Escalante, A. A., Murphy, H., et al. (2019). Integrating environmental and neighborhood factors in MaxEnt modeling to predict species distributions: A case study of Aedes albopictus in southeastern Pennsylvania. *PLoS ONE*, 14(10), 23. <https://doi.org/10.1371/journal.pone.0223821>.
- Wijayanti, S. P., Porphyre, T., Chase-Topping, M., et al. (2016). The Importance of Socio-Economic Versus Environmental Risk Factors for Reported Dengue Cases in Java, Indonesia. *PLoS Negl Trop Dis*, 10(9), e0004964. <https://doi.org/10.1371/journal.pntd.0004964>.
- Wong, M. C., Mok, H. Y., Ma, H. M., et al. (2011). A climate model for predicting the abundance of Aedes mosquitoes in Hong Kong. *Meteorological Applications*, 18(1), 105-110. <https://doi.org/10.1002/met.218>.
- Xiao, J. P., He, J. F., Deng, A. P., et al. (2016). Characterizing a large outbreak of dengue fever in Guangdong Province, China. *Infect Dis Poverty*, 5, 44. <https://doi.org/10.1186/s40249-016-0131-z>.
- Yin, S., Ren, C., Shi, Y., et al. (2022). A Systematic Review on Modeling Methods and Influential Factors for Mapping Dengue-Related Risk in Urban Settings. *International Journal of Environmental Research and Public Health*, 19(22), 15265.
- Yuan, H. Y., Liang, J., Lin, P. S., et al. (2020). The effects of seasonal climate variability on dengue annual incidence in Hong Kong: A modelling study. *Sci Rep*, 10(1), 4297. <https://doi.org/10.1038/s41598-020-60309-7>.
- Zhang, W., Zheng, C., & Chen, F. (2019). Mapping heat-related health risks of elderly citizens in mountainous area: A case study of Chongqing, China. *Science of the total environment*, 663, 852-866. <https://doi.org/10.1016/j.scitotenv.2019.01.240>.

List of tables

- Table 1. The evaluation metrics and criteria for selecting optimal model
- Table 2. Vulnerable groups for dengue fever transmission in Hong Kong.
- Table 3. The selected models with evaluation metrics.
- Table 4. PCA analysis on vulnerable groups

List of figures

- Figure 1. The study area and the locations of positive Ovitrap in the year of 2016 in Hong Kong.
- Figure 2. Workflow of the DF risk mapping
- Figure 3. Results of modeling on the spatial distribution of dengue vector. a) The map for the probability of *Ae. albopictus* presence in Hong Kong; b) Permutation importance of predictor variables; c) Model response curves of 8 environmental factors with permutation importance of over 2%. Red lines show averages after four iterations of the model.
- Figure 4. Maps for dengue fever risk assessment in Hong Kong. a) Local indicators of spatial association of high hazard and high exposure; b) Spatial pattern of vulnerability; c) DF risk assessment map (the areas with the high DF risk level are labeled according to their codes of LTPU).

List of appendices

- Appendix A. Land use map and descriptions
- Appendix B. List for all predictor variables
- Appendix C. Ovitrap location and restricted background for sampling bias
- Appendix D. Correlation between selected predictor variables
- Appendix E. Pareto Frontiers analysis for models
- Appendix F. Spatial autocorrelation between hazard and exposure
- Appendix G. All maps for assessing dengue fever risk
- Appendix H. Underlying factors behind the hot spots for dengue fever risk.

Acknowledgements

This study was funded by the Health and Medical Research Fund by Food and Health Bureau (No. 20190672). S.Y. has got supports from the Hong Kong Scholars Program and Fellowship of China Postdoctoral Science Foundation (No. 2020M672633). We would like to appreciate Mr. LEE Ming Wai from Food and Environmental Hygiene Department (HK) for offering vector surveillance data in Hong Kong.

Figure 1

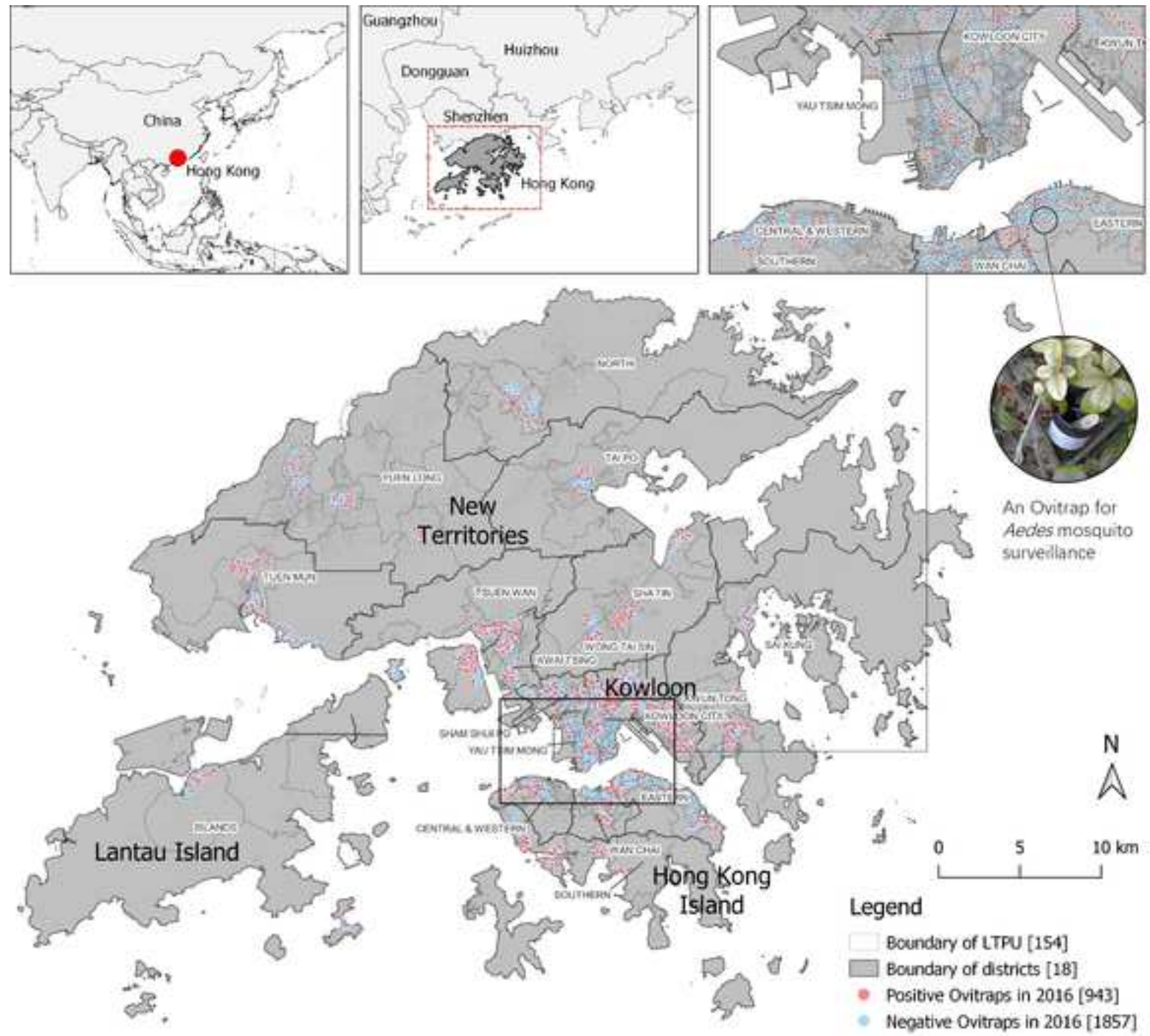


Figure 2

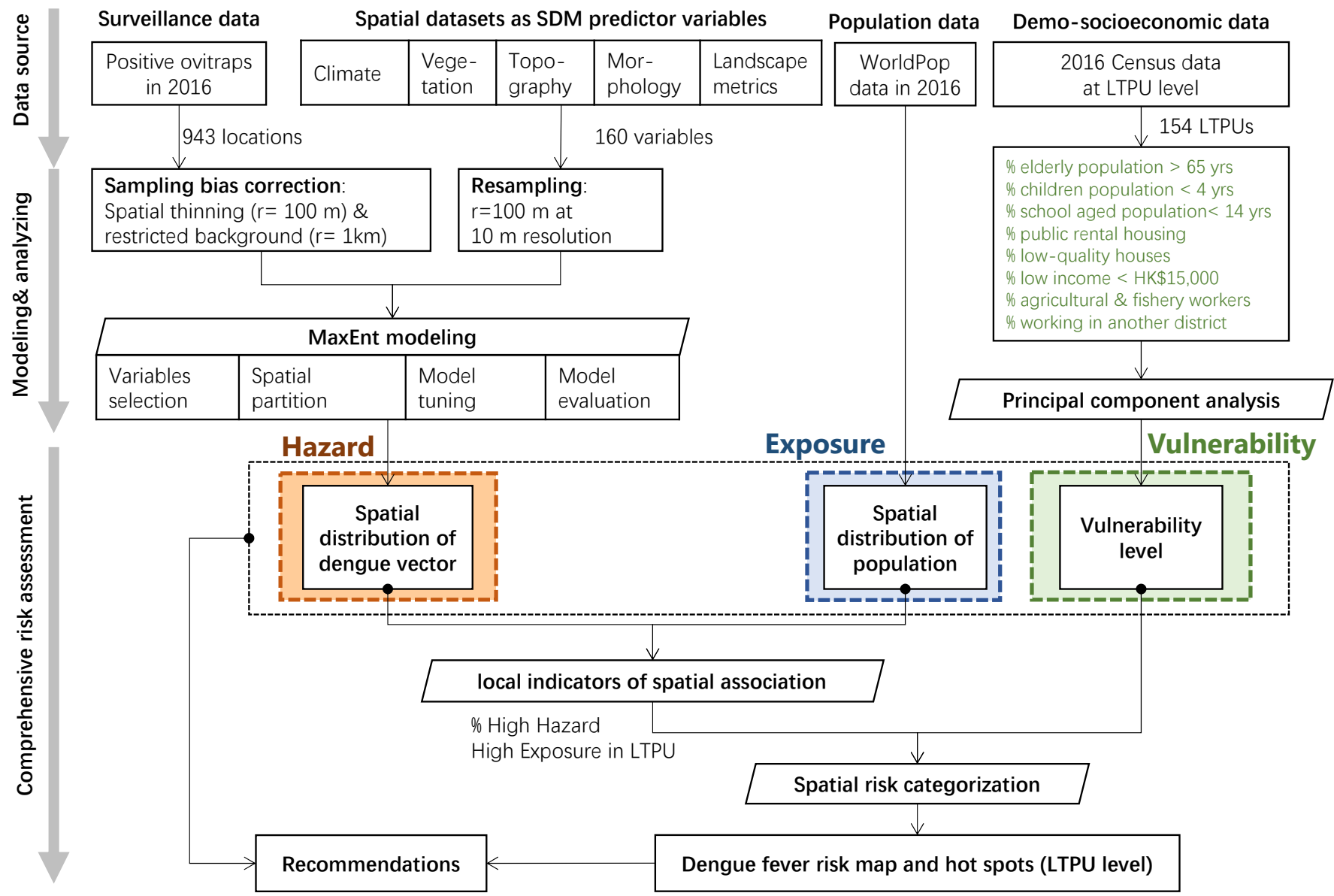


Figure 3

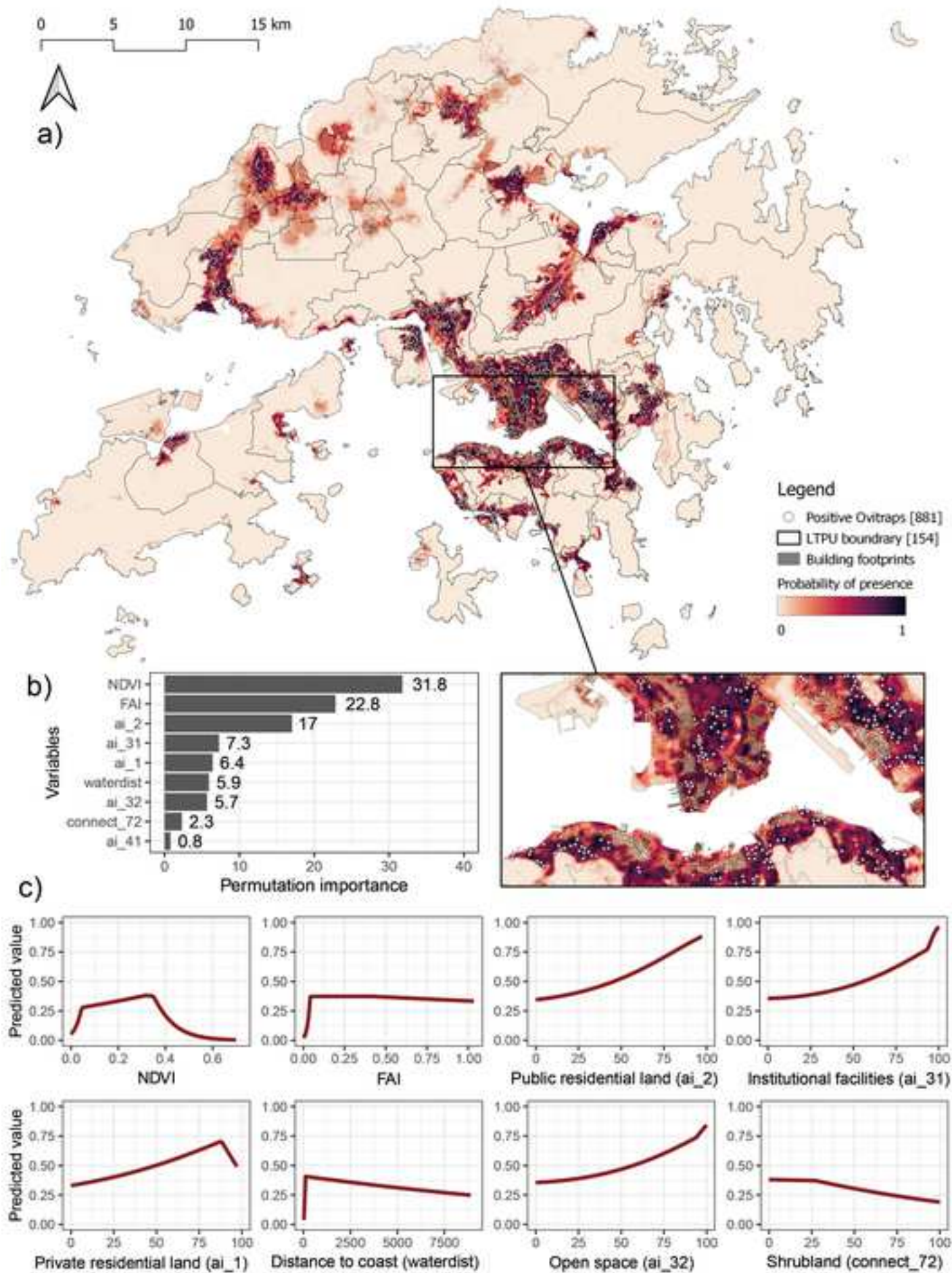
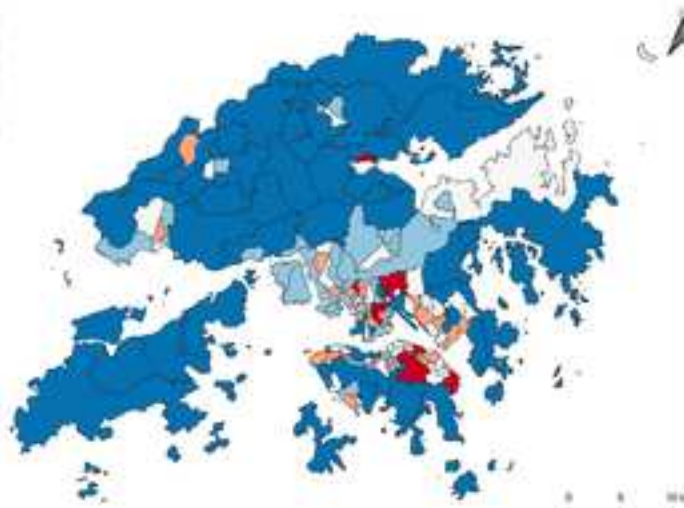
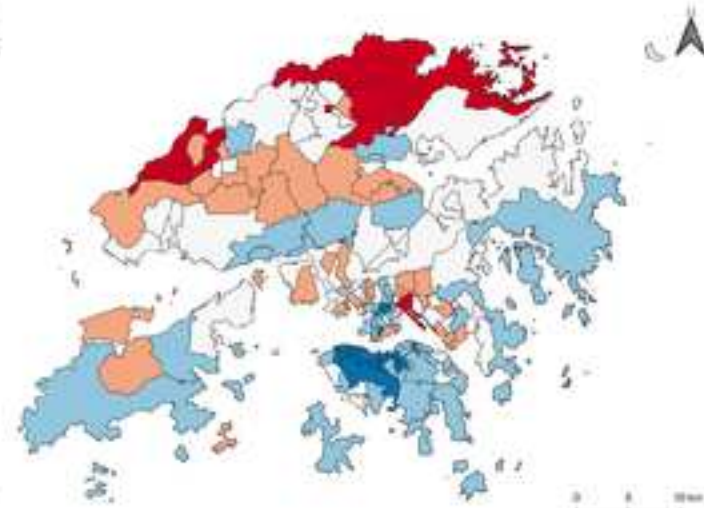


Figure 4

a) %HH



b) Vulnerability



c) Risk

